Tidal effects and the Proximity decay of nuclei

A.B. McIntosh, S. Hudan, C.J. Metelko, and R.T. de Souza
Department of Chemistry and Indiana University Cyclotron Facility
Indiana University, Bloomington, IN 47405

R.J. Charity and L.G. Sobotka
Department of Chemistry, Washington University, St. Louis, MO 63130

W.G. Lynch and M.B. Tsang
National Superconducting Cyclotron Laboratory and Department of Physics and Astronomy
Michigan State University, East Lansing, MI 48824

(Dated: August 10, 2006)

We examine the decay of the 3.03 MeV state of ^{8}Be evaporated from an excited projectile-like fragment following a peripheral heavy-ion collision. The relative energy of the daughter α particles exhibits a dependence on the decay angle of the ^{8}Be*, indicative of a tidal effect. Comparison of the measured tidal effect with a purely Coulomb model suggests the influence of a measurable nuclear proximity interaction.

PACS numbers: PACS number(s): 21.10.Tg, 25.70.Ef

Aggregation of clusters in a dilute medium is a process that impacts a wide range of physical phenomena from the formation of galactic structure to formation of Van der Waals clusters in a low density gas. This aggregation can involve the delicate interplay of elementary forces that results in a frustrated system. One such example is the formation of pasta nuclei in the crust of a neutron star[1, 2]. For smaller systems, the phenomenon of alpha clustering is important both in low density nuclear matter[3], as well as in light nuclei[4]. In the case of heavy nuclei, cluster aggregation is manifested in the spontaneous phenomenon of clusters, from the common process of α decay to the emission of more exotic clusters such as ^{14}C [5]. The reduction of density near the nuclear surface, allows formation of α particles, or other clusters, and their emission from either ground-state or modestly excited nuclei. Cluster emission, thus primarily probes the surface properties of the emitting nucleus[6]. Our present understanding of cluster emission is largely based upon the yields, kinetic energy spectra, and angular distributions of emitted clusters - all of which are well described within a statistical transition-state formalism[7]. In this Letter we present for the first time evidence for the modification of cluster emission by interaction with the nuclear surface. We probe the interaction of the nuclear surface with the emitted cluster by using resonance spectroscopy to examine the emission of ^{8}Be* and specifically explore how its decay is impacted by the tidal effect[8].

Charged particles produced in the reaction ^{114}Cd+^{92}Mo at E/A=50 MeV were detected in an exclusive 4π setup. To focus on evaporated fragments, we selected peripheral collisions through detection of forward-moving projectile-like fragments (PLFs) with $10 \leq Z \leq 48$, in the angular range $2.1^\circ \leq \theta^{lab} \leq 4.2^\circ$ with $\Delta\theta^{Lab} \approx 0.13^\circ$[9]. This PLF is the decay residue of the excited primary projectile-like fragment (PLF*) formed by the collision. Light-charged particles and fragments with $Z \leq 9$ were isotopically identified[9] in the angular range $7^\circ \leq \theta^{lab} \leq 58^\circ$ with the silicon-strip array LASSA [10, 11]. Each of the nine telescopes in this array consisted of a stack of three elements, two 5cm x 5cm silicon strip detectors (Si(IP)) backed by a 2 x 2 arrangement of CsI(Tl) crystals each with photo-diode readout. Each telescope, segmented into 16x16 orthogonal strips, had good angular resolution ($\Delta\theta^{lab} \approx 0.43^\circ$). The 3 x 3 arrangement of the LASSA telescopes was centered at a polar angle $\theta^{lab}=32^\circ$ with respect to the beam axis. The identification threshold of LASSA is 2 MeV/A for α particles. Light-charged particles emitted at other angles were detected by the Miniball/Miniwall 4π phoswich array. For the following analysis events were selected with $15 \leq Z_{PLF} \leq 46$, $V_{PLF} \geq 8.0$cm/ns and the multiplicity of particles in LASSA, $N_{LASSA}=2,3$. Using the measured emitted particles and the assumption of isotropy, the Z, A, and velocity of the PLF* were calculated[12]. For these events the most probable atomic number of the PLF* is ≈ 30.

The kinetic energy spectra of α particles and Be nuclei emitted in the angular range $\theta_{PLF^*} \leq 80^\circ$ are presented in Fig. 1. These spectra are reasonably well described by a Maxwell-Boltzmann distribution supporting the picture of an evaporative process[12]. In comparison to the α particle spectra, the spectra of Be fragments exhibit more pronounced tails indicative of a higher initial temperature[12]. The larger average kinetic energy of ^{7}Be as compared to that of ^{9,10}Be is in agreement with previous work. This difference has been interpreted as the sequential decay of excited primary fragments as they propagate away from the emitting nucleus[9]. For the events presented, damping in the collision process produces a PLF* with a most probable excitation energy of 3 MeV/A and a maximum excitation of 4 MeV/A. The deduced excitation is consistent with the "temperature" associated with the α particle kinetic energy spectra[12].

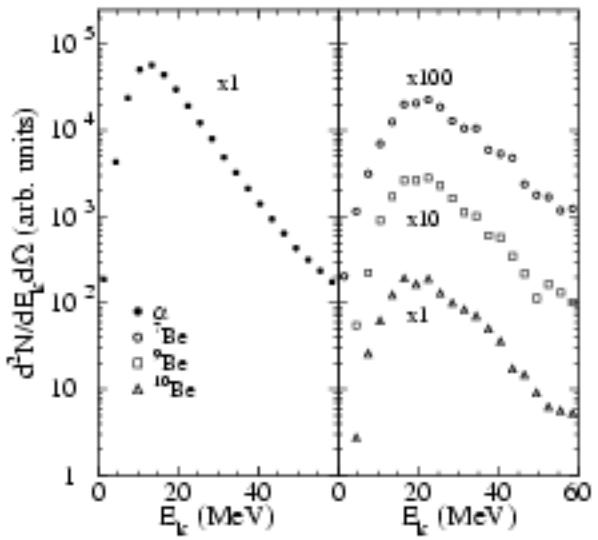

FIG. 1: Kinetic energy spectra of α particles and ^{7,9,10}Be fragments in the PLF* frame observed with $\theta_{PLF^*} \leq 30°$.

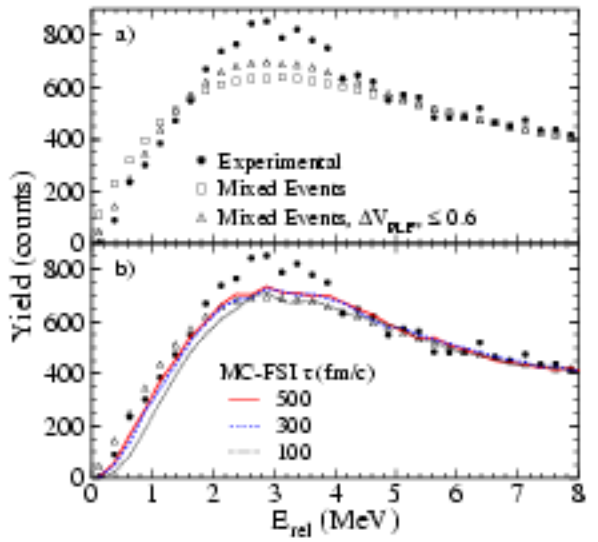

FIG. 2: Panel a: Relative kinetic energy distributions for α-α pairs. Panel b: Comparison of the results of a non-resonant final-state interaction Monte Carlo calculation with the mixed-event background.

The de-excitation cascade of the PLF* involves the emission of not only nucleons and ground state fragments, but also fragments unstable against particle emission.

The decay of short-lived resonant states such as ^{8}Be* can be examined by constructing the relative energy spectrum of the daughter products. Shown in Fig. 2a is the relative energy spectrum between two α particles for events in which either two or three α particles were detected in LASSA with $\theta_{\alpha,PLF^*} \leq 100°$. Solid symbols depict the experimental data which exhibits a peak at $E_{rel} \approx 3$ MeV. The overall shape of the E_{rel} spectrum is affected at low E_{rel} ($\leq$ 2 MeV) by the finite angular acceptance of the LASSA CsI(Tl) detectors, as two particles entering the same CsI(Tl) crystal are not resolved. The ^{8}Be ground-state is consequently not observed in this kinematic regime. For larger E_{rel} ($\geq$5 MeV), the decrease in yield is impacted by the geometric acceptance of LASSA. The observed relative energy distribution can be understood as having two primary components: resonant decay of ^{8}Be* and non-resonant α emission. To assess the non-resonant contribution, which acts as a "background" for the resonant decay, we performed a mixed-event analysis. Two α particles were selected from different events and their relative energy was calculated. The resulting relative energy spectrum was normalized in the interval $14 \leq E_{rel} \leq 50$ MeV and is displayed as open squares in Fig. 2a. While the mixed-event background has the general shape of the observed relative energy spectrum, there is an excess yield in the observed data centered at $\approx$3 MeV. This excess originates from the decay of the first excited state of ^{8}Be at 3.03 MeV with an intrinsic width of 1.5 MeV. Over-prediction of the yield for $E_{rel} \leq 1.5$ MeV is understandable as the mixed-event pairs do not experience Coulomb repulsion. One of the drawbacks of the mixed-event analysis is that the events sampled span a broad distribution of PLF* velocities. To select the conditions that best describe the non-resonant α emission, we restricted the difference in PLF* velocity between two events, ΔV_{PLF^*}, for the events in the mixed-event background. The mixed-event background corresponding to $\Delta V_{PLF^*} \leq 0.6$ cm/ns is shown as open triangles in Fig. 2a. This background provides a better description of the data for $E_{rel} \leq 1.5$ MeV while it exhibits a larger yield at $E_{rel} \approx 3$ MeV. To determine which value of ΔV_{PLF^*} provided the best reproduction of the non-resonant decay, we calculated the χ^2 between the mixed events and the experimental data in the interval $6 \leq E_{rel} \leq 50$ MeV. The minimum χ^2/ν=1.0-1.1 corresponds to ΔV_{PLF^*}= 0.4-0.6cm/ns.

In order to better understand the "background", we have modeled the non-resonant final-state interaction with a Monte Carlo Coulomb trajectory calculation. In this model, which we refer to as MC-FSI, two α particles are emitted in sequential fashion from the surface of an excited nucleus following Lambert emission, while accounting for all recoil and Coulomb interactions. The Z_{PLF^*}, A_{PLF^*}, V_{PLF^*}, and θ_{PLF^*} are taken from the experimental data while the time between emissions is taken to be exponential with a mean time τ. Following Coulomb propagation all particles were filtered for the experimental acceptance, angular resolution, and thresholds. Calculations with τ=100, 300, and 500 fm/c are shown by the lines in Fig. 2b along with the experimental data and mixed-event background. With decreasing mean emission time, suppression of yield for low values of E_{rel} is observed. While the calculation with τ=100 fm/c is clearly inconsistent with the experimental data, $\tau \geq 300$ fm/c provides a reasonable description of the mixed-event background for $E_{rel} \geq 2$ MeV. A deduced mean emission time of this magnitude associated

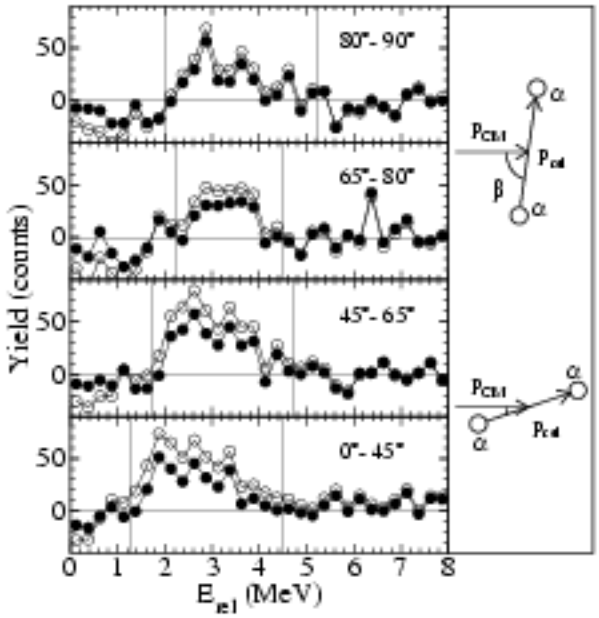

FIG. 3: Difference relative energy spectra of observed α pairs for different decay angles, β, relative to the mixed-event background. Solid symbols depict the spectra using a mixed event background with $\Delta V_{PLF} \leq 0.6$ cm/ns while open symbols correspond to a mixed event background with no ΔV_{PLF} restriction.

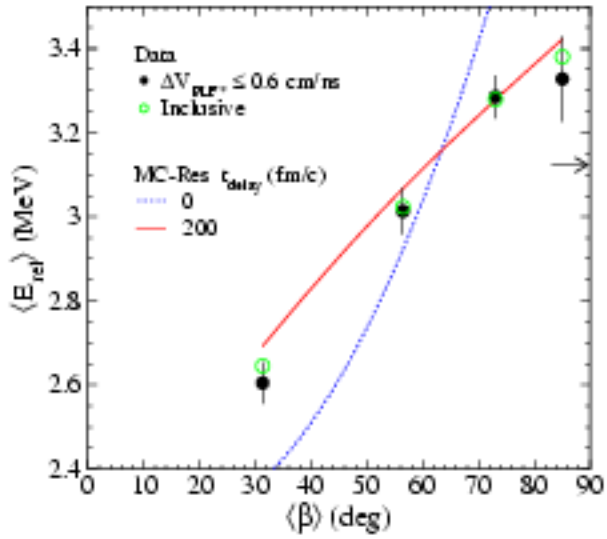

FIG. 4: Dependence of $\langle E_{rel} \rangle$, associated with the two α particles arising from the decay of first excited state of ^{8}Be, on the average decay angle, $\langle \beta \rangle$. Lines represent the results of Monte Carlo calculations for resonance decay.

with an excitation energy of 3 MeV/A is consistent with previous work[13]. For smaller values of E_{rel}, mutual Coulomb repulsion of the two α particles results in a suppression of yield at small E_{rel} as compared to the mixed-event data. The comparison of the mixed-event background with the Monte Carlo final state calculation indicates that for all but the smallest values of E_{rel} the mixed-event background provides a reasonable description of the non-resonant contribution.

The first excited state of ^{8}Be has an intrinsic width of 1.5 MeV[14] corresponding to a mean lifetime of $\approx$131 fm/c. For such a short lifetime the likelihood that this state decays in the vicinity of the emitting nucleus is significant. Consequently, as the ^{8}Be* decays into two α particles, its increasing quadrupole moment interacts with the gradient of the Coulomb field. For α pairs which decay orthogonal to the emission direction, the field gradient provided by the emitting nucleus acts to increase their relative energy. In contrast, α pairs which decay along the emission direction experience a reduced relative energy due to the larger acceleration of the nearer α particle[8]. In order to examine this Coulomb tidal effect, we constructed the difference relative energy spectra of the observed α pairs relative to the mixed-event background. These spectra were constructed for different decay angles, β, calculated as the angle between the relative momentum of the α-α pair and the center-of-mass momentum of the pair. Depicted as the solid symbols in Fig. 3 is the case using the mixed-event background with $\Delta V_{PLF} \leq 0.6$ cm/ns. For reference, the difference spectra with no restriction on ΔV_{PLF} are also shown as open symbols. Clearly the ΔV_{PLF} restriction does not introduce a major change in the difference relative energy spectra. The prominent feature of the difference spectra is the peak at $\approx$3 MeV which is evident for all β. Moreover, it is clearly evident that the peak in the difference spectrum for $0 \leq \beta \leq 45°$ is shifted to lower values of E_{rel} as compared to larger values of β. To quantitatively extract the dependence of $\langle E_{rel} \rangle$ on β for the 3.03 MeV state, we integrated the difference spectra over the region indicated by the vertical lines. These integration limits were selected by considering the intrinsic width of the 3.03 MeV state and the shape of the measured spectra. The extracted $\langle E_{rel} \rangle$ is largely insensitive to any reasonable choice of integration limits. Using the difference spectra associated with $\Delta V_{PLF} \leq 0.6$ cm/ns, we extract a measured yield of the ^{8}Be of 1063 counts. Accounting for the detection efficiency of two α particles as compared to a Be we deduce a yield for the 3.03 MeV state in this kinematic region of 4252 counts. In the same kinematic region the measured yield of ^{7,9,10}Be isotopes is 5337,6727, and 4559 respectively. If we assume the total yield of ^{8}Be is 6000 counts and a temperature of 5 MeV the resulting population of the 3.03 MeV state is $\approx$4400 counts. Thus, the measured yield for the 3.03 MeV state is in reasonable agreement with the measured yields for ^{7,9,10}Be.

The dependence of the average relative energy, $\langle E_{rel} \rangle$, on the decay angle β is shown in Fig. 4 as solid symbols. A clear manifestation of the tidal effect is observed as $\langle E_{rel} \rangle$ increases with increasing β. The magnitude of the observed change in $\langle E_{rel} \rangle$ is $\approx$0.7 MeV, a relative change of $\approx$25%. For reference, the arrow indi-

cates the decay energy corresponding to the intrinsic energy of the state and the Q-value of the decay. The error bars shown, while dominated by the measurement statistics, include the uncertainty associated with the integration limits. To demonstrate the sensitivity of $<E_{rel}>$ to different mixed-event backgrounds we also show as open symbols the dependence of $<E_{rel}>$ on β for no restriction on ΔV_{PLF4}. The same overall trend of $<E_{rel}>$ on β is observed for the different mixed-event conditions.

To understand this observed trend quantitatively, we simulated the decay of a $^8Be^4$ in a simple Monte Carlo model, MC-Res. In this model the $^8Be^4$ is emitted isotropically from the surface of the PLF^4. The properties of the PLF^4 were sampled in the same manner as in the MC-FSI calculations. The lifetime of the emitted $^8Be^4$ was chosen consistent with an exponential probability distribution $P(t)=\exp(-t/\tau)$, reflecting first order kinetics. The mean lifetime, τ, was taken to be 131 fm/c determined by the intrinsic state width. The initial kinetic energy of the $^8Be^4$ is taken to be exponential with a slope parameter of 7.5 MeV, consistent with the experimental data shown in Fig. 1. The $^8Be^4$ propagates in the Coulomb field of the emitting nucleus until it decays. At the moment of decay the $^8Be^4$ is replaced with two α particles with an inter-α separation distance (scission configuration) given by $R_{\alpha-\alpha}$= 5.81 fm in accordance with systematics[15]. The kinetic energies of the two α particles respect conservation of total energy and momentum. Selecting a smaller inter-α separation, namely $R_{\alpha-\alpha}$= 4 fm, makes a negligible difference in the final results. The decay angle, β, of the two α system with respect to the emission direction is taken to be isotropic namely the effect of the Coulomb field in orienting the decaying $^8Be^4$ is neglected. Following decay, the two α particles are propagated along trajectories corresponding to both the Coulomb repulsion from the PLF^4 and their mutual Coulomb repulsion. Energy and momentum are conserved at all stages of the calculation. Particles are subsequently filtered by the detector acceptance, angular resolution, and thresholds.

The results of this schematic calculation are shown as the dashed line in Fig. 4. The angular dependence of $<E_{rel}>$, namely the magnitude of the tidal effect, is clearly overestimated by the purely Coulomb calculation. One possible reason for this difference is the interaction of the emitted $^8Be^4$ with the nuclear surface. This interaction is particularly important as the most probable initial velocity of the $^8Be^4$ is close to zero, and consequently the $^8Be^4$ spends a significant time within the range of the proximity interaction. This is in marked contrast to the tidal decay following projectile breakup reactions[16]. The attractive surface interaction can impact the decay of the evaporated $^8Be^4$ in two ways. It can stabilizes the $^8Be^4$ while it is in the vicinity of the emitting nucleus. In addition, the attractive potential may produce a *nuclear* tidal effect with the *opposite sign* as compared to the Coulomb tidal effect. Both the nuclear tidal effect and the increased stability of the $^8Be^4$ will result in a decreased dependence of $<E_{rel}>$ on β. To assess whether nuclear attraction could be responsible for the difference between the observed tidal effect and the Coulomb calculation, we have introduced a delay into the decay time distribution such that $P(t)=\exp(-(t-t_{delay})/\tau)$ for $t>t_{delay}$. This artificial delay mimics the increased stability of the $^8Be^4$ due to the nuclear interaction. With increasing t_{delay}, the dependence of $<E_{rel}>$ on β decreases as evident in Fig. 4. For t_{delay}=200 fm/c, represented by the solid line, one observes reasonable agreement with the observed tidal effect. Without any delay the lifetime of 131 fm/c corresponds to a decay distance of $\approx$17 fm. For t_{delay}=200 fm/c, the $^8Be^4$ travels on average an additional 4 fm before decaying. From this we conclude that stabilization of the $^8Be^4$ by the emitting nucleus for a distance of $\approx$4 fm is sufficient to reproduce the magnitude of the observed tidal effect. A more realistic model of the nuclear interaction is necessary in order to extract more quantitative results.

In summary, we have measured the dependence of $<E_{rel}>$ on decay angle for the first excited state of ^8Be. This trend can be understood as a tidal effect in which the decaying cluster interacts with the gradient of an external field provided by the emitting nucleus. Calculations with a Coulomb model over-predict the observed tidal effect. This over-prediction suggests that the emitting nucleus influences the cluster decay through the nuclear interaction. The attractive nuclear potential of the emitting nucleus acts to both stabilize the excited cluster and induces a nuclear tidal effect which opposes the Coulomb tidal effect.

Acknowledgments

We would like to acknowledge the valuable assistance of the staff at MSU-NSCL for providing the high quality beams which made this experiment possible. This work was supported by the U.S. Department of Energy under DE-FG02-88ER40404 (IU), DE-FG02-87ER-40316 (WU) and the National Science Foundation under Grant No. PHY-95-28844 (MSU).

[1] D. G. Ravenhall et al., Phys. Rev. Lett. 50, 2066 (1983).
[2] C. J. Horowitz et al., Phys. Rev. C 69, 045804 (2004).
[3] G.Ropke et al., Phys. Rev. Lett. 80, 3177 (1998).
[4] A. Tohsaki et al., Phys. Rev. Lett. 87, 192501 (2001).
[5] H. J. Rose and G. A. Jones, Nature 307, 245 (1984).
[6] L. G. Sobotka and R. J. Charity, Phys. Rev. C 73, 014609 (2006).
[7] L. G. Moretto, Nucl. Phys. A. 247, 211 (1975).

[8] R. J. Charity et al., Phys. Rev. C. 63, 024611 (2001).
[9] S. Hudan et al., Phys. Rev. C 71, 054604 (2005).
[10] B. Davin et al., Nucl. Instr. and Meth. A473, 302 (2001).
[11] A. Wagner et al., Nucl. Instr. and Meth. A456, 290 (2001).
[12] R. Yanez et al., Phys. Rev. C. 68, 011602(R) (2003).
[13] L. Beaulieu et al., Phys. Rev. Lett. 84, 5971 (2000).
[14] D. R. Tilley et al., Nucl. Phys. A. 745, 155 (2004).
[15] L. G. Sobotka et al., Phys. Rev. Lett. 51, 2187 (1983).
[16] R. J. Charity et al., Phys. Rev. C. 52, 3126 (1995).